

Introduction to the Integrated Brace Flexibility Compensator Viscous Fluid Control Device for Structures

Mehdi Ahmadizadeh, PhD¹

Abstract

This paper presents a comprehensive introduction to the formulation and potentials of a novel structural control device known as the Integrated Brace Flexibility Compensator (IBFC). This device has been developed by the author and its development was partially published in a number of reports and theses. The IBFC is a semi-active viscous fluid damper that works by applying control forces that tend to minimize the brace flexibility effects. It is shown that in addition to the well-established advantages of semi-active control devices over their passive or active counterparts, the proposed control device offers additional advantages, including i) the ability to work independently of other control devices in the structure, ii) requiring minimal information about structural properties for design, iii) requiring little structural response measurement, iv) reduced dependence of design to the stiffness of bracing elements, and v) a performance similar to that of more detailed semi-active devices that are based on active control theory.

Keywords

Structural control; semi-active control; brace flexibility; integrated compensation

Introduction

Active structural control systems are expected to outperform passive systems in obtaining the desired seismic response. However, passive control systems have gained more popularity [1] mainly due to their inherent stability, independence from external power sources, lower cost, and ease of use and maintenance. Furthermore, it has been shown that the performance of passive viscous fluid control systems are usually less sensitive to changes in structural properties due to nonlinearity or modeling and estimation errors [2]. Semi-active control has been developed to bridge the gap between active and passive control devices by improving the performance over passive systems with little energy requirement and by ensuring structural stability using fail-safe implementation techniques. These control devices take advantage of an active control algorithm to determine the desired control force at any

¹ Department of Civil Engineering, Sharif University of Technology, PO Box 11155-4313, Azadi St, Tehran, Iran
Email: ahmadizadeh@sharif.edu

instance, and then produce a control force that is closed to the desired value to the possible extent, by actively changing the properties of a passive device (e.g. modifying the orifice size in a viscous fluid damping device). Several studies have shown the performance advantages of these systems over passive ones, but mostly only when the compared passive system has the minimum or maximum value of damping that is possible in semi-active mode [3]. However, Ahmadizadeh [3] showed that such comparisons may be inadequate, as the optimum value of passive device damping coefficient is not necessarily equal to the minimum or maximum possible values. By examining the optimum passive damping properties for viscous fluid dampers as components of a supplemental energy dissipation system, it was shown [3] that passive systems can lead to structural performances that are very close to those achieved by semi-active systems, mainly due to the lower- and upper-bound limitations of control force in semi-active systems. Furthermore, it was demonstrated that the majority of the performance improvement obtained using semi-active viscous fluid dampers originates from the mitigation of the brace flexibility effects in the generated control force, rather than the active control algorithm.

Based on the findings of Ahmadizadeh [3], a simple semi-active control algorithm has been developed and presented herein that works merely by reducing the effects of brace flexibility. The proposed control device, named Integrated Brace Flexibility Compensator (IBFC) only uses a local feedback signal and does not rely on any active control algorithm. This device was originally developed by author and was partially introduced in several publications [3-5]. In this paper, the IBFC device is thoroughly presented along with the underlying formulation, usage examples and future potentials.

The Integrated Brace Flexibility Compensator (IBFC) Device

The IBFC device is a semi-active viscous fluid damper whose damping constant is modified by a relation to reduce the effects of the connected brace.

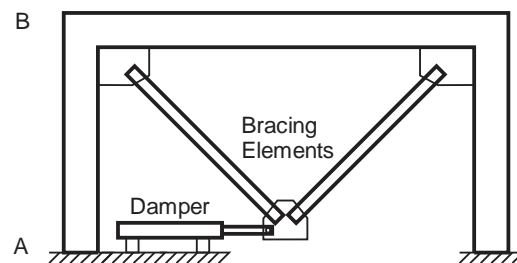


Figure 1 A story equipped with a damper connected through bracing elements

Formulation

A typical structural story equipped with a damper is shown in Figure 1. This damping device along with its arm and connecting bracing elements can be modelled using a Maxwell model shown in Figure 2. In this figure, C_d is the damping coefficient of the device, and K_a and K_b are the stiffness of damper arm and the effective stiffness of bracing elements and their connections, respectively. As shown, all coefficients are used after they are projected to the horizontal direction.

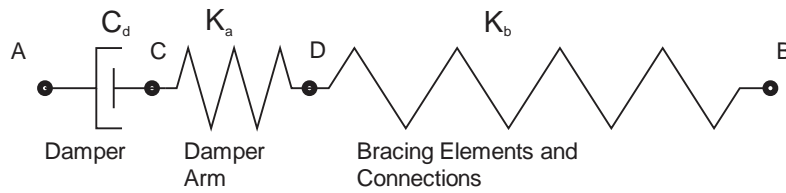


Figure 2 Mathematical model for the damping device and connected bracing elements

To fully eliminate the effect of brace flexibility, the damper should work as if point C in Figure 2 is directly and rigidly connected to point B at the top of the story. In this case, the velocity that the damper shaft experiences will be equal to the interstory velocity, implying a purely viscous behavior and a fully rigid brace. The damper force can then be obtained from:

$$F_d(t) = C_{d0}V_s(t) \tag{1}$$

where $V_s(t)$ represents the interstory velocity, i.e. velocity of point B relative to point A, and C_{d0} is a constant linear damping coefficient. To obtain a similar force in practice, a semi-active damper can be employed whose force is governed by:

$$F_d(t) = C_d(t)V_d(t) \tag{2}$$

and then equating the resulting force with that of Equation 1. This yields the following equation for instantaneous damping coefficient of the device [3]:

$$C_d(t) = C_{d0} \frac{V_s(t)}{V_d(t)} \tag{3}$$

In the above equations, $V_d(t)$ is the device shaft velocity, i.e. the velocity of point C relative to point A. In Equation 3, C_{d0} is a coefficient that should be optimized for the structure in question. It should be noted that the damping coefficient resulting from this equation can only be used when it is positive and less than the maximum possible damping coefficient. Equation 3 in its current form requires the instrumentation of the story and device to determine their velocity ratio. The IBFC alleviates this requirement by using a dynamic strain gauge on the damper arm as shown in Figure 3 through the following derivation.

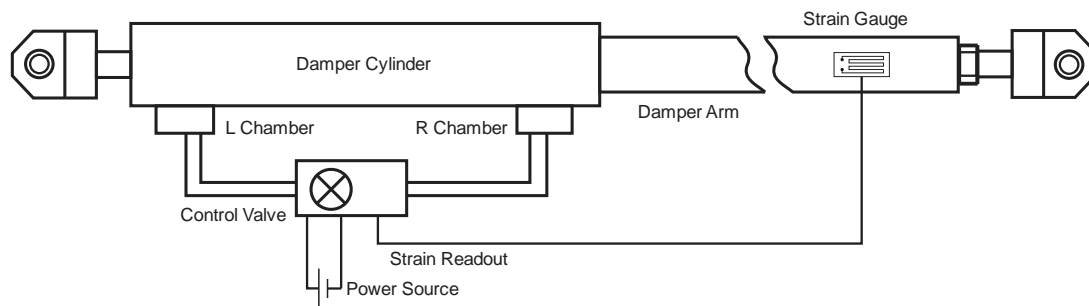


Figure 3 IBFC with a dynamic strain gauge installed on damper arm

The damper arm stiffness is governed by:

$$K_a = \frac{A_a E_a}{L_a} \tag{4}$$

where A_a , E_a and L_a are damper arm cross-sectional area, modulus of elasticity and length, respectively. The force developed in damper can then be obtained from:

$$F_d(t) = K_a \Delta L_a(t) = A_a E_a \varepsilon(t) \quad 5$$

in which ΔL_a is the damper arm elongation and $\varepsilon = \frac{\Delta L_a}{L_a}$ is the strain readout from the strain gauge. Knowing that the damper viscosity and arm stiffness work in series, the force developed in them $F_d(t)$ obtained by Equations 2 and 5 must be equal at all times. In addition, the relative velocities of components should satisfy:

$$V_s(t) = V_d(t) + V_a(t) + V_b(t) \quad 6$$

where $V_a(t)$ and $V_b(t)$ represent the relative velocities of the ends of the damper arm (between points C and D) and the bracing elements (between points D and B), respectively. Next, to write each of these velocity components in terms of the stress readout from damper arm, one can use Equation 5 to write:

$$V_d(t) = \frac{F_d(t)}{C_d(t)} = \frac{A_a E_a}{C_d(t)} \varepsilon(t) \quad 7$$

and:

$$V_b(t) = \lim_{\Delta t \rightarrow 0} \frac{\Delta L_b}{\Delta t} = \lim_{\Delta t \rightarrow 0} \frac{\Delta F_d / K_b}{\Delta t} = \lim_{\Delta t \rightarrow 0} \frac{A_a E_a \Delta \varepsilon(t) / K_b}{\Delta t} = \frac{A_a E_a}{K_b} \dot{\varepsilon}(t) \quad 8$$

where $\dot{\varepsilon}(t)$ is the rate of change of arm strain. The arm velocity can also be written as:

$$V_a(t) = \lim_{\Delta t \rightarrow 0} \frac{\Delta L_a}{\Delta t} = \lim_{\Delta t \rightarrow 0} \frac{L_a \Delta \varepsilon(t)}{\Delta t} = L_a \dot{\varepsilon}(t) \quad 9$$

Substituting these velocity expressions into Equation 6:

$$V_s(t) = \frac{A_a E_a}{C_d(t)} \varepsilon(t) + \left(\frac{A_a E_a}{K_b} + L_a \right) \dot{\varepsilon}(t) \quad 10$$

Furthermore, combining Equations 3 and 7 yields:

$$V_s(t) = \frac{C_d(t) V_d(t)}{C_{d0}} = \frac{A_a E_a}{C_{d0}} \varepsilon(t) \quad 11$$

Equations 10 and 11 can then be solved to obtain an expression for $C_d(t)$:

$$C_d(t) = \frac{C_{d0}}{1 - \frac{C_{d0}}{K_{eq}} \dot{\varepsilon}(t)} \quad 12$$

in which $K_{eq} = 1 / \left(\frac{1}{K_b} + \frac{L_a}{A_a E_a} \right)$ is the combined stiffness of damper arm and bracing elements. It should be noted that the above equation is valid as long as the device damping coefficient $C_d(t)$ has not reached zero. When any singularity occurs in the calculation of Equation 12, the default damping constant C_{d0} should be used.

As shown, the only input to determine the suitable semi-active damping coefficient in Equation 12 is strain and its first time derivative. The parameter C_{d0} is in fact the design parameter that should be optimized to obtain the best structural performance. The optimum value of this constant is expected to be close to those for ordinary linear damping devices connected to flexible bracing elements. However, this will lead to better energy dissipation and reduced absolute acceleration response, as will be shown later in the numerical studies.

In practice, an online analog circuit can use Equation 12 along with the necessary calibration coefficients to simply convert the voltage read from the strain gauge to the command voltage necessary for a servovalve that regulates the damping coefficient for the device, in which case, the delay will be minimized. In digital applications, by using finite difference equations and accepting a small delay, the rate of change of strain can be obtained from:

$$\dot{\varepsilon}(t) \approx \dot{\varepsilon}(t - \Delta t/2) = \frac{\varepsilon(t) - \varepsilon(t - \Delta t)}{\Delta t} \quad 13$$

which further simplifies the damping coefficient expression to:

$$C_d(t) = \frac{C_{d0}}{1 - \frac{C_{d0}}{K_{eq}\Delta t} \left(1 - \frac{\varepsilon(t - \Delta t)}{\varepsilon(t)}\right)} \quad 14$$

Advantages of the IBFC Device

Considering Equations 12 or 14, the IBFC device can be observed to have the following advantages over customary semi-active control devices:

- i. The IBFC device does not need an active control algorithm in its control logic, minimizing the required amount of online calculations. This, in turn, leads to reduced delay between response detection and application of control force, further improving the resulting performance.
- ii. The performance of the IBFC is based on a single local instrumentation readout, making it independent of the other devices present in the structure. Furthermore, the design will be less dependent on the dynamic properties of the structure (similar to a passive device and in contrast with active control systems), which makes it less prone to performance degradation as a result of modeling or estimation errors.
- iii. Overall, fewer design parameters, reduced instrumentation requirements, and little processing needs makes this device simpler than many other semi-active control devices.

In addition, as will be shown later in numerical simulations, the proposed IBFC device can lead to structural performances that are very close to those obtained from customary semi-active systems; these systems usually take advantage of active control algorithms and are controlled by a central processor to determine the control force based on overall instantaneous structural response.

Limitations of the IBFC Device

Similar to other semi-active control devices, the IBFC device has a damping coefficient that is limited to its minimum (non-negative) and maximum values. These are usually governed by the maximum velocity for which the orifices and valves are designed, and the maximum output force that can be safely endured by damper arm and bracing. Particularly, the fact that the damper force direction is always governed by the direction of its local excitation, reduces the ability of semi-active dampers to effectively emulate an active control algorithm on the structure as shown in Ref. [3], or even their ability to fully alleviate the effects of brace flexibility. In addition, measurement noise needs to be removed from the strain readouts to ensure a stable performance of the damper.

Numerical Studies

To study the behavior of the IBFC device and validate the performance advantages that were sought in the above development, the force-velocity-displacement behavior of this damper is first compared to that of ordinary linear viscous fluid dampers. Then, the results of previous studies are used and extended to demonstrate the performance advantages of proposed control device. Finally, the actual performance of this device is validated through a case study of an actual controlled building structure.

Force-Displacement-Velocity Behavior of the IBFC

First, consider an ordinary linear passive viscous fluid damper installed in a single-story structure using a flexible brace as shown in Figure 1. In this example, a 2% inherent damping is assumed for the structure, its mass is assumed to be 200 metric tons, and story stiffness is chosen to result in a natural fundamental period of vibration of 0.4 seconds. The bracing elements used to connect the damper are assumed to result in a lateral stiffness equal to that of the story. For simplicity, the damper arm is assumed to be rigid and all flexibility is assumed to be originating from the brace.

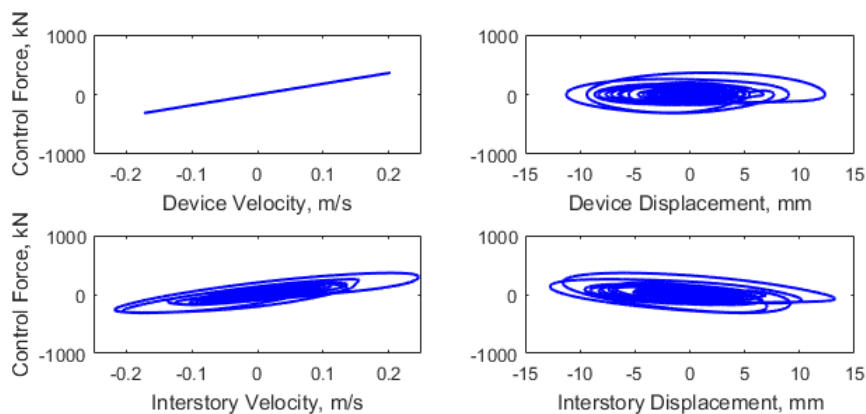


Figure 4 Force developed in an ordinary linear passive viscous fluid damper with respect to device and interstory velocity

Using a performance index that is the same as that of Ref. [3], an optimum constant damping coefficient of 1.8 kN-s/mm can be found for this configuration. The force-velocity-displacement relationship of this device-brace assembly when the structure is subjected to El Centro earthquake excitation is shown in Figure 4. It can be observed that while the damper itself behaves linearly, the device-brace assembly behaves as if this combination has a reduced damping coefficient (based on a reduced overall slope of the force-velocity diagram of the damper-brace assembly) and degraded energy dissipation performance (through reduced area enclosed within the force-displacement diagram). In fact, this behavior is a direct result of the phase lag of the device velocity with respect to the interstory velocity, as illustrated in Figure 5.

Next, the passive device is replaced by an IBFC device with the same value for C_{d0} , and the analysis results are presented in Figure 6. The minimum and maximum values of damping coefficients are limited to 0 and 100 kN-s/mm, respectively. In addition, the setting time for

the damper valve to enforce the desired damping coefficient is assumed to be 0.1 s without any overshoot. In this manner, the damping coefficients will trail the desired values, as is expected in the dynamic behavior of mechanical devices.

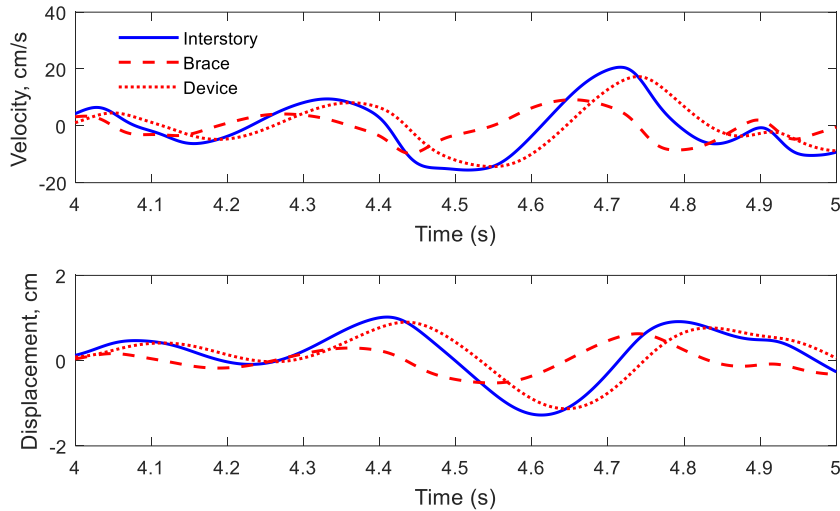


Figure 5 Histories of story, brace and device displacement and velocity for linear passive damper.

Figure 6 shows that while the damper behavior is nonlinear and rather complicated, the force-velocity relation of the damper-brace assembly has become slightly closer to linear, indicated by its trend and orientation that somewhat follows a linear curve. Of course, a full linear behavior cannot be achieved here due to the semi-active damper limitations that were discussed earlier in this paper. Considering the force-displacement relation shown in the same figure, one can observe that the apparent elasticity of the brace-damper assembly has been reduced as a result of the reduction of the effects of brace flexibility.

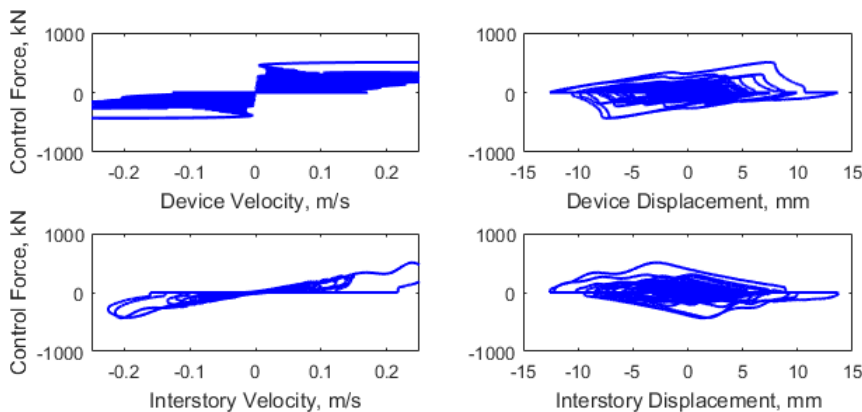


Figure 6 Force developed in IBFC with respect to device and interstory velocity and displacement

From a structural performance standpoint, only replacing the passive damper with the equivalent IBFC device is observed to reduce the acceleration response by more than 5%. An increase in energy dissipation is also observed by about 4%. A further optimization of the IBFC

leads to a better acceleration performance improvement of 7% at C_{d0} value of 1.6 kN-s/mm, which corresponds to an energy dissipation improvement of about 5%.

Another way to achieve the above-mentioned improvement in energy dissipation is using a passive linear damper with a damping coefficient of 1.6 kN-s/mm along with a brace that is three times as stiff as the original brace. While energy dissipation by a control device does not necessarily lead to a better structural performance [1], this analogy shows the success of the proposed control logic in the mitigation of the effects of brace flexibility on its energy dissipation performance.

Structural Performance Effects

While the concept of IBFC was originally introduced by author in Ref. [5], several other studies by this author and his colleagues have been carried out that demonstrate the important role of the reduction of brace flexibility effects in achieving better structural performance. In this section, a summary of most notable studies is presented and extended to demonstrate the structural performance effects of the IBFC device. Where necessary, the readers are referred to appropriate references for more detail.

Controlled Structural Response Spectra

Ahmadizadeh [3] demonstrated that a semi-active control system that is merely based on the reduction of brace flexibility effects performs nearly as well as a semi-active control system based on LQR algorithm. To further demonstrate this, the results of parametric studies on single-degree-of-freedom and two-degree-of-freedom systems with passive, active and semi-active control systems are presented here. The natural periods of the systems are selected to range from 0.2 s to 3.0 s. With a mass of 200 metric tons (equally distributed for the two-degree-of-freedom system), the appropriate story stiffness has been selected for each desired fundamental natural period of vibration. The uncontrolled system is assumed to have an inherent damping of 2% of critical. The device damping coefficient is allowed to range from 0 to 100 kN-s/mm, with the maximum produced force being limited to 700 kN. Four ratios of the brace stiffness to the story stiffness, namely 1, 2, 4, and 8, have been considered.

For each set of the period and brace stiffness values, the peak drift and absolute acceleration responses of the uncontrolled system when subjected to 1940 El Centro earthquake are first determined, which are simply the linear displacement and absolute acceleration response spectra for 2% damping. Then, an optimal passive control system is chosen, whose damping coefficient is within the above-mentioned range. To find the optimal damping coefficients, the same performance index as that of Ref. [3] is minimized for each analysis case with equal weights for displacement and acceleration responses. Then, this procedure is repeated for each of the other considered control strategies, namely LQR active, LQR semi-active, and IBFC. The latter control device is termed semi-active based on interstory velocity (ISV) in the following graphs for more clarity. In the above systems, the design variables are either the weighting matrices in the LQR performance index [7], or the constant damping coefficient C_{d0} of the control device. Full state feedback with minimal uncompensated delay is assumed in all analyses.

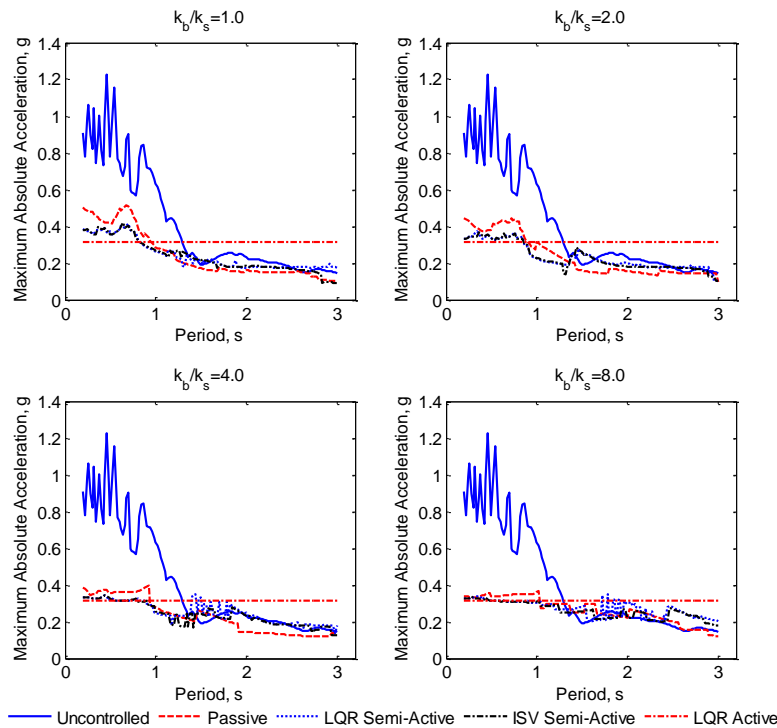


Figure 7 Controlled response spectra of single-degree-of-freedom system - accelerations.

Single-Degree-of-Freedom Systems

The controlled response spectra for the single-degree-of-freedom systems are shown in Figures 7 and 8. It can be observed that while all control strategies significantly reduce the structural response, as expected, the best performance belongs to the active control system. Active control essentially makes the system act as a rigid body, despite the above-mentioned limitations on the control force; the drifts are negligible, and accelerations are very close to the peak ground acceleration. It should be noted that with selection of different structural performance indices or weights, one can achieve a variety of drift-acceleration response combinations using this approach based on the design objective.

Figures 7 and 8 demonstrate that the performances achieved by the LQR semi-active, ISV semi-active, and optimum passive systems are very close. In fact, the two semi-active control systems result in almost identical structural performances; the LQR control algorithm seems to have almost no effect in improving the performance of the structure through a semi-active system.

It is evident that the need for the removal of the brace flexibility effect will be less with larger brace stiffness values. As a result, the performances of the considered control systems become closer with stiffer braces. Particularly, semi-active systems show very little performance improvement over the optimum passive system for the highest considered brace-to-story stiffness ratio. Rather than the utilized control algorithm, this further supports the role of brace flexibility compensation in improving structural performance using semi-active devices.

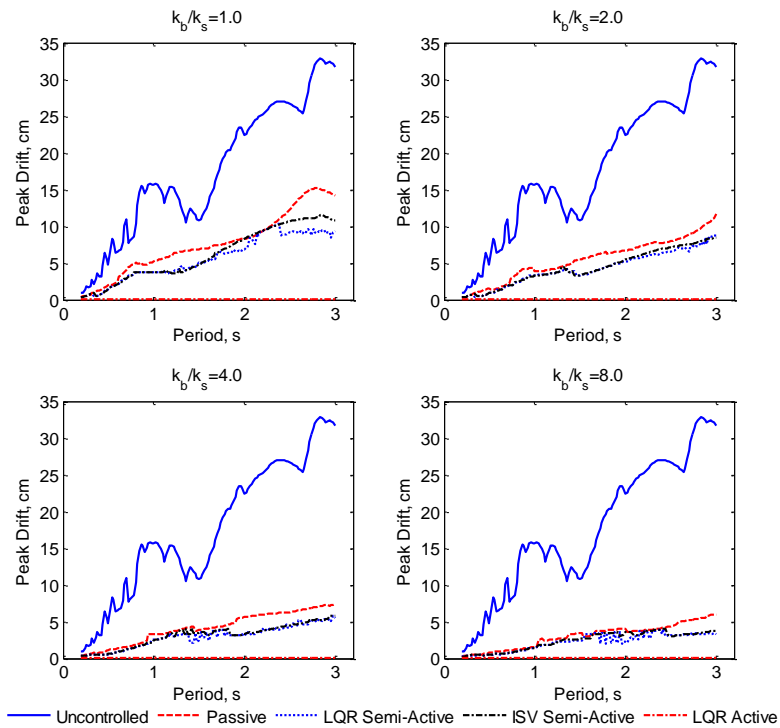


Figure 8 Controlled response spectra of single-degree-of-freedom system - accelerations.

Two-Degree-of-Freedom Systems

Two cases have been considered in the parametric study of two-degree-of-freedom systems: i) with only one device and bracing elements in the lower floor, and ii) with both stories equipped with devices and bracing elements.

In case i, where only first story is equipped with a control device, the active control system results in a performance closer to the other ones, as shown in Figure 9. Nonetheless, this control strategy still outperforms other systems: the drifts are smaller in long periods, and the accelerations are significantly reduced in lower periods. LQR control system takes advantage of full state feedback to calculate the control force, and therefore, is able to adjust this force to reduce the peak response of the second story as well as the first story, although no control force is being directly applied to the second story.

Although the performance achieved by LQR semi-active system is slightly better than the optimum passive system in the same manner, it does not significantly surpass the improvement resulting from semi-active system based on interstory velocity. Considering that the latter does not use any active control algorithm, this observation again supports the above statement on limited ability of the semi-active system in applying the control forces governed by the control algorithm. Rather, the semi-active systems appear to be merely able to reduce the effects of brace flexibility on the performance.

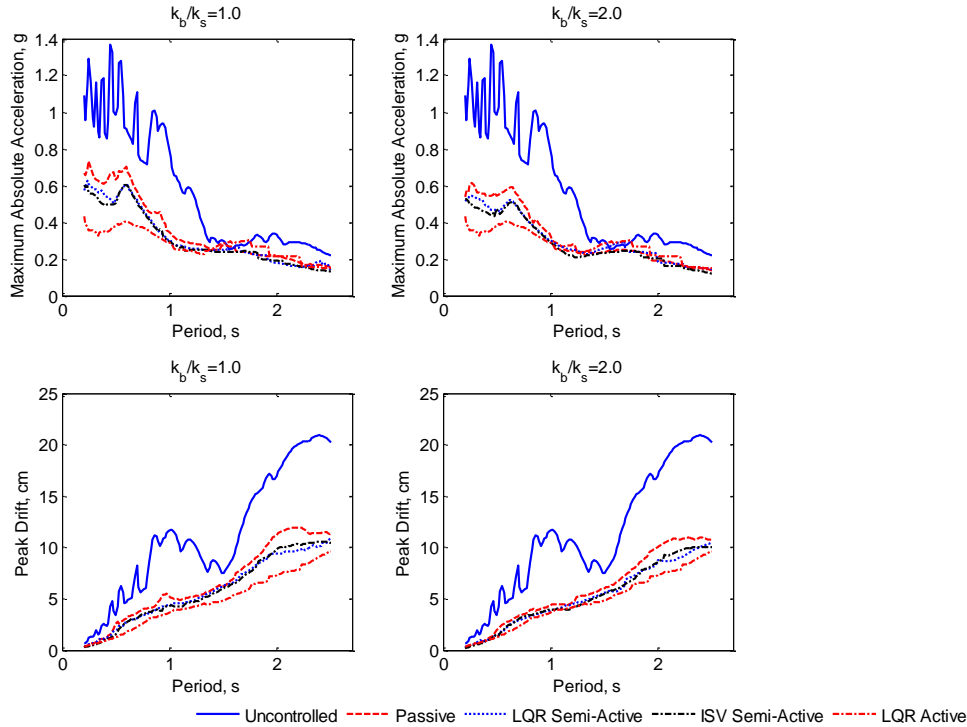


Figure 9 Controlled response spectra of two-degree-of-freedom system with one device in the first story.

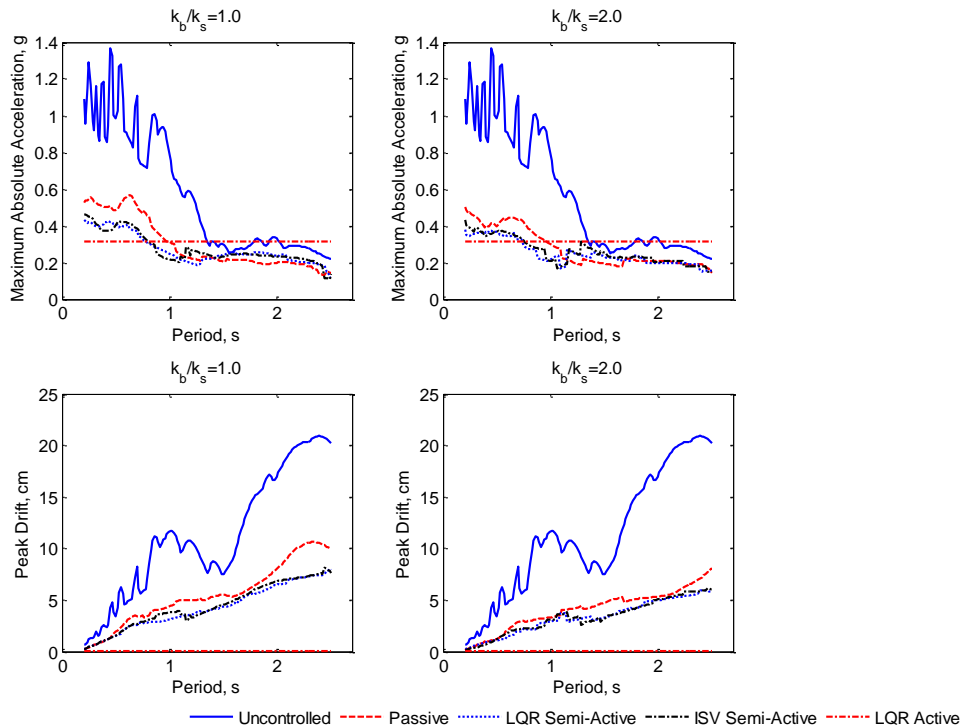


Figure 10 Controlled response spectra of two-degree-of-freedom system with devices in both stories..

The same conclusions can be drawn from case ii, in which control devices are assumed to be present in both stories (Figure 10). However, in this case, the LQR active control system is again able to make the structure act similar to a rigid body, while the LQR semi-active system

does not demonstrate any considerable advantage over the semi-active system based on interstory velocity.

Table 1 Structural response reductions in parametric studies.

Structure	k_b/k_s	Average peak response reductions (% of uncontrolled response)							
		Passive		LQR semi-active		ISV semi-active		LQR active	
		Drift	Accel.	Drift	Accel.	Drift	Accel.	Drift	Accel.
1DOF	1	57.0	45.6	68.1	53.7	66.0	53.6		
	2	68.2	49.3	76.0	58.5	75.3	58.3		
	4	75.7	53.4	82.4	58.5	81.5	58.7	99.5	55.5
	8	82.2	52.8	86.5	55.9	85.6	56.2		
2DOF with 1 device	1	41.9	40.6	47.3	48.2	49.3	49.6		
	2	47.5	46.9	52.8	52.5	53.9	54.2		
	4	51.7	51.9	55.5	56.1	56.0	57.0	57.8	62.2
	8	54.5	55.5	56.5	58.4	56.9	58.0		
2DOF with 2 devices	1	50.9	50.1	60.8	62.3	59.4	62.3		
	2	62.1	57.3	68.7	66.8	69.3	65.1		
	4	69.4	61.5	76.0	67.1	75.3	66.6	98.4	66.6
	8	75.7	64.9	80.3	66.3	79.6	68.4		

Table 1 summarizes the numerical results obtained from the above parametric studies. The percentages show average reductions of response quantities from those of the uncontrolled structure over the considered period range. However, the period range is limited to 0.2 to 1.2s for calculation of accelerations, as beyond this period range, acceleration responses are small, and their variations are insignificant. In summary, one can observe that the IBFC device performs very well merely based on interstory velocity, and LQR control algorithm has limited effect on the performance when used as a control logic for semi-active systems.

Case Study

In addition to the above-mentioned parametric studies, Ahmadizadeh [3] also showed that the ISV semi-active system is sufficient to result in a performance similar to that of an LQR semi-active system in the first actual usage of semi-active devices in a building in Japan [6]. Here the results of Ref. [3] are presented with the addition of active control as a possible control alternative.

The Building configuration and its dynamic properties are shown in Figure 11 and Table 2, respectively. The maximum device force is limited to 900 kN here, and the variable damping coefficients for each of the devices are assumed to range from 0 to 200 kN-s/mm. Two devices are installed in each of the lower four stories of the building as shown in Figure 11. The equivalent stiffness column of Table 2 is calculated based on the fact that the stiffness of the brace and device are in series. An inherent damping of 2% is assumed for the structure.

Based on the dynamic properties of the considered structure, the first mode period of the uncontrolled building is 0.992 s. The semi-active control system was originally designed by Kurata et al. [6] using LQR algorithm, the details of which can be found in Ref. [7]. The uncontrolled peak response of the structure under 1940 El Centro earthquake is compared to peak responses with various control strategies in Figure 12. To ensure a reasonable

comparison, each of these control systems have been individually designed to result in the best performance, observing the limitations on damping coefficients and control forces. As shown in this figure, all control strategies reduce the peak responses by almost the same amounts.

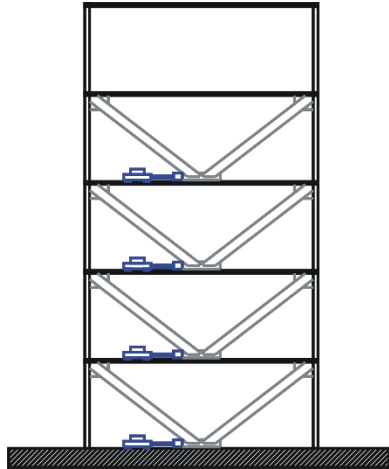


Figure 11 Case study structure [6]

Table 2 Dynamic properties of case study structure

Floor	Mass (kg)	Story stiffness k_s (kN/mm)	Brace stiffness k_b (kN/mm)	Device stiffness k_d (kN/mm)	Equivalent stiffness k_{eq} (kN/mm)
5	266 100	84	--	--	--
4	204 800	89	565×2	400×2	234.2×2
3	207 000	99	565×2	400×2	234.2×2
2	209 200	113	565×2	400×2	234.2×2
1	215 200	147	438×2	400×2	209.1×2

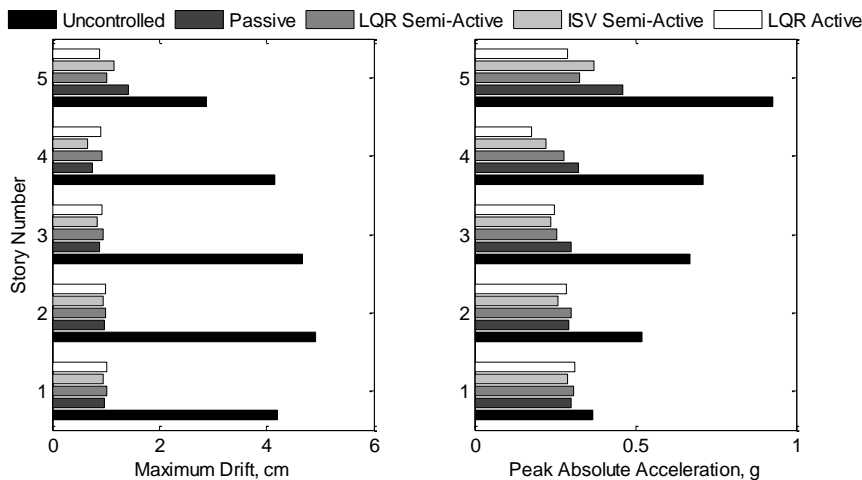


Figure 12 Peak response of case study building subjected to El Centro earthquake

It is important to note that in this case study, an optimum passive control system is achieved with damping coefficients set to only 4% of their maximum values. When the maximum damping coefficients are used for the passive mode, the drifts are observed to be reduced

while accelerations show larger values than the uncontrolled building – similar to the behavior of a rigidly braced building. In the extreme case of very large damping coefficient, the effective fundamental period of the structure reduces to 0.61 s, which is closer to the dominant periods of most earthquakes.

Simulations using stronger earthquakes have also shown that the same structural performance conclusions can be drawn. For example, 1995 Kobe earthquake results demonstrate that the passive and the semi-active systems perform similarly under this earthquake. The first-floor control device force history of the considered control systems in these simulations are shown in Figure 12. It is evident that the control force differences between these control strategies are very small, implying that the optimal LQR controller tends to resemble a force history similar to that of an optimal passive system with a rather stiff brace.

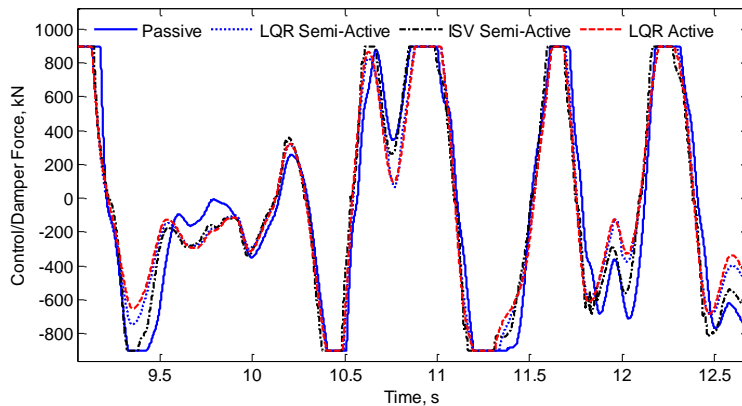


Figure 13 Control and damper force histories in the first floor of case study building subjected to 1995 Kobe earthquake

Future Developments

Study is already underway to design a *passive* control device that tends to reduce the brace flexibility effects [4]. From special design of orifice geometry, or orifices that are resized in response to oil pressure and oil or damper arm velocity, to utilization of the energy applied to the damper to make the damper independent of external power sources, several possibilities are being considered to enhance the design. A passive or at least a self-contained semi-active damping device would be very desirable for structural applications due to its ease of design and implementation, with performances that were shown to be close to semi-active systems that employ active control algorithms.

Conclusions

The Integrated Brace Flexibility Compensator (IBFC) control device was introduced and shown to be capable to significantly improve the structural performance. Particularly, it was shown that the resulting performance can be very similar to those obtained using semi-active systems that employ active control algorithms.

The IBFC was shown to have significant advantages over ordinary passive and semi-active systems. Most notably, compared to passive devices, this device offers improved performance and reduced design dependence on the stiffness of connecting bracing elements; compared to active and other semi-active control systems, advantages of the IBFC include decentralized operation, minimal instrumentation and processing requirements, independence from active control algorithms, and reduced reliance on structural properties for design and operation.

References

1. Christopoulos, C. and A. Filiatrault, *Principles of Passive Supplemental Damping and Seismic Isolation*. 2006, Pavia: University of Pavia.
2. Khansefid, A. and M. Ahmadizadeh, *An investigation of the effects of structural nonlinearity on the seismic performance degradation of active and passive control systems used for supplemental energy dissipation*. *Journal of Vibration and Control*, 2015.
3. Ahmadizadeh, M., *On equivalent passive structural control systems for semi-active control using viscous fluid dampers*. *Structural Control and Health Monitoring*, 2007. **14**(6): p. 858-875.
4. Kheyri, F. and M. Ahmadizadeh, *Design and Modeling of an Improved Passive Viscous Damper Based on the Reduction of the Effects of Brace Flexibility (MSc thesis in Persian)*, in *Department of Civil Engineering*. 2015, Sharif University of Technology: Tehran, Iran.
5. Rasoulnia, A. and M. Ahmadizadeh, *Development of an Improved Semi-active Damper Based on the Reduction of the Effects of Brace Flexibility (MSc thesis in Persian)*, in *Department of Civil Engineering*. 2012, Sharif University of Technology: Tehran, Iran.
6. Kurata, N., et al., *Actual seismic response controlled building with semi-active damper system*. *Earthquake Engineering & Structural Dynamics*, 1999. **28**(11): p. 1427-1447.
7. Soong, T.T., *Active Structural Control: Theory and Practice*. 1990, New York: Longman.